Water Resources Research

RESEARCH ARTICLE
10.1029/2018WR023338

Identifying Wetland Consolidation Using Remote Sensing in the North Dakota Prairie Pothole Region

Christopher Krapu[1], **Mukesh Kumar**[1,2,3], **and Mark Borsuk**[1]

[1]Department of Civil and Environmental Engineering, Duke University, Durham, NC, USA, [2]Nicholas School of the Environment, Duke University, Durham, NC, USA, [3]Department of Civil, Construction and Environmental Engineering, University of Alabama, Tuscaloosa, AL, USA

Key Points:
- The North Dakota portion of the Prairie Pothole Region has experienced substantial changes to the area-perimeter relations of its water bodies
- Wetland consolidation measured via area-perimeter relations covaries strongly with changes in land use
- The timing of consolidation coincides substantially above-average precipitation, suggesting a potential landscape-wide hysteretic effect

Supporting Information:
- Supporting Information S1

Correspondence to:
M. Kumar,
mukesh.kumar@ua.edu

Citation:
Krapu, C., Kumar, M., & Borsuk, M. (2018). Identifying wetland consolidation using remote sensing in the North Dakota Prairie Pothole Region. *Water Resources Research*, *54*. https://doi.org/10.1029/2018WR023338

Received 21 MAY 2018
Accepted 10 SEP 2018
Accepted article online 19 SEP 2018

Abstract Artificial drainage of wetlands in the Great Plains has been linked to increased runoff, erosion, and the consolidation of small, seasonal wetlands into larger, more permanent bodies of water. We analyzed hydrologic changes to over 1.2 million water bodies across the entire North Dakota portion of the Prairie Pothole Region using the ratio of aggregate water area and total perimetric length in a landscape-scale shape index calculated from existing Landsat derived data of water presence/absence. This ratio showed a clear change point toward more consolidation of wetlands around the period 1999 (±1 year) after an extended multiyear period of above-average rainfall. We used hydrologic simulations with forcing data from across the region to show that this shift is unlikely to be due solely to natural variation in precipitation and evapotranspiration. Using county-level regressions, we found that wetland consolidation as measured by the shape index was highly correlated with agricultural transitions out of wheat and into corn and soybeans over the period 1984–2014 ($R^2 > 0.4$), though we do not find evidence of a strong correlation between reported drainage and wetland consolidation. These results highlight a potential hysteretic interaction involving interannual variations in hydrologic forcing and anthropogenic landscape alterations on wetland consolidation in the North Dakota prairie potholes.

Plain Language Summary We measured the area and perimeter of a large number of water bodies in the North Dakota prairies using satellite imagery and found evidence of a clear break in their usual relationship around the year 1999 following a period of above-average rainfall. The magnitude of this change appears to be related to changes in agricultural practices across the region. These findings suggest that the behavior of wetland systems can change abruptly at large scales as a result of human-climate interactions.

1. Introduction

The Prairie Pothole Region (PPR) of central North America extends over four U.S. states and three Canadian provinces. It is named for the large number of small *pothole* depressions left over from the Wisconsin glaciation, which retreated from this area approximately 11,500 years ago (Bluemle, 2016). These potholes lack continuous surface connections to the stream network and therefore tend to accumulate water. While the climate of the region is relatively dry with less than 600 mm of annual rainfall, much of it falls as snow, and spring meltwater is typically the largest source of replenishment for the wetlands within these basins. These wetlands provide a range of ecosystem services including habitat for migratory waterfowl (Kantrud et al., 1989), flood mitigation and retention (Huang et al., 2011), and sequestration of atmospheric carbon (Euliss et al., 2006). Furthermore, they have been the focus of extensive restoration and preservation efforts (Paradeis et al., 2010) to protect their recreational and ecological value in the face of increasing pressure from modern agriculture to convert them into productive farmland. Artificial drainage of wetlands for agriculture is not limited to central North America and is common in places such as the coastal plain of the Netherlands, the tropical peatlands of southeast Asia (Verhoeven & Setter, 2010), and across eastern Europe (Hartig et al., 1997). The desire to reclaim wetlands for arable land is one of the foremost reasons for wetland conversion globally (van Asselen et al., 2013). The vulnerability of PPR wetlands to conversion is at least partially due to their geometry and basic morphological features. Wetland basins in the PPR are relatively shallow with low slopes and flat bottoms and are dependent on snowmelt and groundwater recharge for replenishment (Hayashi et al., 2016). Their volume-to-area ratios are relatively low, making them ideal candidates for cost-effective drainage in the form of surface ditches or subsurface pipes. However, this also makes them productive habitats for aquatic invertebrates and the animals that feed upon them (Cox et al., 1998). Furthermore,

their shallow depth makes them susceptible to substantial drawdowns during drought, leading to a highly dynamic environment supporting a high degree of biodiversity (Johnson et al., 2010). These dynamics are driven by interactions between atmospheric conditions and groundwater reservoirs, leading to oscillation between wet and dry conditions. Substantial variations across space and time lead to a range of different wetland hydroperiods ranging from ephemeral and temporary wetlands to permanently flooded ponds and lakes. The region undergoes wet-dry cycles marked by transitions between cool, drier weather and warmer, wetter weather (Johnson et al., 2004; Todhunter, 2016). Since prairie wetlands undergo exchange with the local groundwater table, there exists a strong coupling between wetland water levels and climate variability (LaBaugh et al., 2016).

Ongoing monitoring of the health and viability of wetland ecosystems is an issue of concern for U.S. wetlands in general (Cohen et al., 2016; Creed et al., 2017). Rapid changes in land use (Wright & Wimberly, 2013) across the U.S. interior impart a sense of urgency to data analyses of prairie wetlands with the goal of identifying trends (Dahl, 2014) or abrupt changes to either their number or spatial pattern. In light of recent debate regarding the suitability of existing regulation to protect wetlands within the context of federal law (Calhoun et al., 2017; Leibowitz et al., 2018; Reynolds et al., 2006), substantial attention should be given to the current rate of wetland consolidation and the factors driving their change. The wetlands of the PPR and in North Dakota in particular present an opportunity to study the ongoing conversion of wetlands into cropland. A similar process is known to have happened much earlier to the south and west in states such as Iowa and Ohio. These drainage efforts were largely complete by 1965 (Pavelis, 1987), precluding the use of remote sensing for tracking wetland change in these places. The North Dakota PPR is an ideal site to study the interaction between land use and wetland hydrodynamics because of ongoing changes to the agricultural practices of the region.

Demand for biofuels and livestock feed is known to drive wetland conversion in the states of North and South Dakota (Johnston, 2013) amidst a shift in crop type from small grains such as wheat and barley to soybeans and corn over the past half-century (Johnston, 2014). The mechanisms linking agriculture to wetland decline and disappearance are well explored in the existing literature (Kessler & Gupta, 2015; McCauley, Anteau, & Post van der Burg, 2015; Wiltermuth & Anteau, 2016), and the general consensus is that both surface and subsurface drainage installations cause a decrease in the number of small wetlands in terms of volume and ponded area, with an accompanying increase in the water volume stored in downstream receiving basins (Anteau, 2012). Agricultural drainage is attractive to landowners for a variety of reasons. Waterlogged soils tend to depress yields for important crops such as corn, wheat, and soy, while ponds and wetlands in the middle of fields can be converted to productive farmland with sufficient drainage. Drainage installation is hypothesized to follow periods of increased soil moisture in the PPR over the past two decades (McKenna et al., 2017) as farmers seek to prevent wet soils from limiting crop yields. The net effect of this hydrological manipulation appears to be a reduction in the total amount of shoreline habitat (Anteau, 2012), which subsequently affects wetland ecology.

One of the main benefits provided by PPR wetlands is the habitat they provide for waterfowl, which depend upon the region for feeding and reproduction. Hunting and other recreational activities associated with waterfowl are a primary source of value derived from these wetlands (Leitch & Hovde, 1996). Wetlands' suitability for supporting wildlife appears to be heavily dependent upon the range of dynamic variation in water levels, which is naturally suppressed in larger bodies of water (Anteau, 2012) exhibiting a reduced perimeter-to-area ratio. Therefore, wetland function depends on the amount of shoreline habitat available.

Characterization of prairie wetland size distributions and shifts in these distributions has been a fruitful and vigorous area of research (Christensen et al., 2016; Serran et al., 2018; Steele & Heffernan, 2017; Van Meter & Basu, 2015; Zhang et al., 2009) with the understanding that anthropogenic modification often leads to preferential loss of smaller wetlands. Smaller wetlands are already at higher risk of emptying due to relatively high lateral outflows to groundwater per unit area (Hayashi et al., 2016). While this makes them effective sources of recharge to the local groundwater table, it also means that climate and human-derived effects on pothole wetland size distributions may be confounded. It is apparent that drained water bodies will have reduced water levels, and there is substantial evidence that drainage can increase overall water surface areas for the remaining downstream basins (McCauley, Anteau, van der Burg, et al., 2015). Artificial drainage can therefore lead to the disappearance of water bodies while simultaneously increasing the total area of nearby wetlands and ponds.

Attribution of wetland changes on a broad scale may be difficult, as periods of drought are confounded with decreasing wetland water levels due to drainage, while above-average precipitation will be confounded with ponded area expansion due to drainage. Furthermore, increases in precipitation can lead to merging of two or more wetlands into a combined wetland of a different type, potentially leading to apparent *losses* if working strictly from counts of water bodies (Kahara et al., 2009). A dimensionless and scale-free statistic of wetland geometry is therefore desirable, and a shape index defined in terms of perimeter and area is occasionally used in other spatial analysis contexts (McGarigal & Marks, 1994). Van Meter and Basu (2015) incorporated an analysis of changes in shape index in the Des Moines Lobe portion of the PPR, finding that contemporary wetlands tend to have more simplified geometries relative to historical wetlands. Merendino and Ankney (1994) used shape index as one of several descriptors of wetland fertility in the context of duck reproductive success.

In this work, we offer new information regarding the timing and intensity of alterations to wetland hydrology by monitoring surface water using remote sensing over the period 1984–2014. We consider the existence of ponded water to be a prerequisite for wetland presence and use ponded extent as a proxy for wetland size. Our goal is to further the understanding of the spatiotemporal dynamics of wetland habitat in the PPR over the past 30 years by answering the following research questions:

1. Are changes in wetland shape index more reflective of wetland drainage or interannual variation in climate?
2. When did substantial shifts in wetland shape index occur in the North Dakota portion of the PPR?
3. Are changes in wetland shape index related to agricultural change?

In general, our strategy is to analyze groups of wetlands by recognizing that artificial drainage leads to expansion and shrinking of wetlands within close proximity and that this local variance in hydrologic behavior is atypical of natural filling-drying cycles. This assumption is predicated on conservation of mass and does not hold in areas where wetlands can be drained into streams or rivers. Our methodology includes hydrologic surrogate simulations as well as observational analysis. We discuss a generalization of the shape index to a multiobject setting (section 2.1) and show by simulation (section 2.2) that it is invariant with regard to changes in wetland water volume caused by natural variations in precipitation. Section 2.3 outlines an analysis of the North Dakota portion of the PPR using this landscape-level shape index to identify the most likely dates and intensity of changes to wetland shape index. We apply this analysis at a per-county level in section 2.4 to relate intensity of shifts in wetland shape index to existing data on agricultural practices and drainage. Finally, we discuss the limitations (section 2.5) and results (section 3) of our approach and integrate the results from all three previous sections in the discussion section (section 4) and relate our findings to the existing base of knowledge on prairie wetlands. While our findings are necessarily restricted to the PPR, we note that the methods used are applicable to any region with large numbers of wetlands, which exhibit dynamic variation in water levels and ponded area. Since wetlands with shallow, gently sloping basins undergo a greater change in ponded area relative to steeper ones for a unit change in water volume, these approaches are best suited for locations with low relief.

2. Methodology

2.1. Measuring and Simulating Wetland Area and Perimeter

Given that wetland function depends on dynamic variation in water levels and the amount of shoreline habitat, it is informative to compute a metric relating this area to the total amount of water present in a wetland. While multiple terminologies exist, the term shape index is often used (McGarigal & Marks, 1994) to refer to a quantity (1) proportional to the square root of a shape's area (a) divided by its perimeter (p). Van Meter and Basu (2015) found that agricultural drainage in Iowa leads to measurable changes in the shape index S commensurate with decreased perimeter-area ratios.

$$S \propto \frac{\sqrt{a}}{p} \tag{1}$$

As area has dimensions of length^2 while perimeter has dimensions of length^1, S is dimensionless and does not suffer from a scale dependency as does the perimeter-area ratio, which has dimensions of length^{-1}. A

generalization of the shape index to multiple patches is the landscape shape index (LS) (Patton, 1975) defined as

$$\mathrm{LS} = \frac{\sqrt{\sum_{i=1}^{n} a_i}}{\sum_{i=1}^{n} p_i} \tag{2}$$

where i indexes one of 1, …, n patches or shapes considered. This quantity retains the dimensionless property of (1) and provides an aggregate measure of compactness of shapes as well as the number that are present. Consequently, uniform expansion or contraction of all water bodies in a region will have little impact upon LS.

To tabulate changes in LS, we extend the above framework, noting that if LS is held constant, then there is a linear relationship $\sqrt{A} = f(P)$ where $\sqrt{A} = \sqrt{\sum_{i=1}^{n} a_i}$ and $P = \sum_{i=1}^{n} p_i$ are the sums of areas and perimeters over n wetlands. Supposing that there is a structural change between two different functional relations f_1, f_2, that is, this relationship changes at some point in time, we measure the difference between f_1 and f_2 as $\overline{f_2 - f_1}$ averaged over 100 points in the interval $[P_{\min}, P_{\max}]$ where $P_{\min}$ and $P_{\max}$ denote the minimum and maximum over time of P in a given landscape unit. Finally, $\overline{\sqrt{A}}$ is the arithmetic mean of $\sqrt{\sum_{i=1}^{n} a_i}$ over all years. We combine these terms in equation (3) to create a quantity which covaries with area-perimeter ratios in a scale-free fashion. We will refer to this as the consolidation score S_C .We adopt the convention that the term f_2 denotes a postchange relation, while f_1 denotes a prechange relation. Therefore, S_C is a measure of the distance between the two lines in Figure 4, normalized by the total area of surface water on the landscape.

$$\mathrm{S_C} = \frac{\overline{f_2 - f_1}}{\overline{\sqrt{A}}} \tag{3}$$

We posit that changes in *LS* encapsulated in rising values of S_C are reflective of artificial drainage of wetland ponded areas for two reasons. First, water bodies with simplified geometries with higher area-perimeter ratios offer more compact storage of water volumes per unit surface area and therefore maximize the amount of land available for agriculture. Long, snaky water bodies are a major obstacle toward efficient use of farmland. Second, a major objective of wetland drainage is to eliminate wet depressions altogether and prevent water from ponding, leading to a reduced wetland count n. Both of these impacts are expected to lead to positive values of S_C. We also posit that *LS* should not change substantially with natural drought-deluge cycles as these tend to simply enlarge or shrink existing all ponded areas within a region and therefore affect their scale without substantially altering their geometry. Since S_C is dimensionless and therefore scale-free, it appears to be an ideal metric of wetland consolidation that is robust against natural expansion and shrinkage of wetlands and ponds due to variations in forcing. A key assumption within this work is that S_C will not change appreciably due to climatological variations.

These variations have the effect of altering the groundwater table and therefore introducing positive or negative inputs to large numbers of wetlands simultaneously. These groundwater fluxes correspond to movements along the wetland continuum (Euliss et al., 2004) and typically do not correspond to anthropogenic effects, though they may shift wetlands between alternate states (Mushet et al., 2018). A key assumption within this work is that S_C will not change appreciably with movements along the groundwater axis of the wetland continuum, which correspond to, on average, uniform increase or contraction of wetland ponded area within the vicinity of the changing groundwater table. In simpler terms, this is the assumption that increasing the groundwater table cannot lead to wetland emptying if all other relevant quantities are held constant and that our measure of consolidation is zero despite changes to the groundwater table. To test the hypothesis that $S_C = 0$ under natural conditions, we conducted hydrologic simulations, as discussed in the next section.

2.2. Hydrologic Simulations

To determine whether S_C covaries with precipitation or drainage, we conducted hydrologic simulations of landscape units containing wetlands with simplified, circular geometries both with and without connections established by agricultural drainage. We used forcing time series of precipitation and temperature from the North Dakota PPR over the period 1980–2010 to capture interannual variation in these climate variables.

These simulations are not intended to exactly reflect any specific set of existing wetlands but rather to further our understanding of an idealized system. We followed the procedure laid out in Huang et al. (2013) for implementing a conceptual pothole water storage model of wetland water volume at a daily time step as a function of hydroclimatic inputs and basin properties. While the original model incorporated realistic basin geometries from remote sensing, we only considered circular conical basins to allow for efficient simulation of a wide range of drainage scenarios and to eliminate the effect of shifts in wetland elongation and shape complexity on our results. Additionally, we omitted an additive term originally included in Huang et al. (2013) corresponding to an empirical adjustment as our implementation of this model was not calibrated to observational data. The processes represented include snowpack accumulation, snowmelt runoff, direct precipitation onto the ponded area, storm runoff, ponded surface evaporation, and shallow groundwater loss due to ET in the wetland periphery.

In this wetland hydrology model, wetland ponding corresponds to filling of the bottom of the basin and so the ponded area and contributing upstream area sum to the total catchment area. Each landscape unit of 1,000 wetlands was driven using forcing data from one of these 10 locations (Table S1). We then also allowed for drainage, controlled by the parameter P_{drain}. This parameter defines the annual probability that a wetland is irreversibly drained in a year. About 100 landscape-level simulations of 1,000 wetlands each were conducted for each value of P_{drain} from the set {0.00,0.05,0.10, …0.5}. As we allowed drainage only in 1 year (year 16 out of 30), P_{drain} can also be interpreted as the proportion of wetlands, which were drained in each simulation. The first 5 years were simulated to spin-up the system from an empty state, while years 6–16 and 16–26 served as predrainage and postdrainage evaluation periods for calculation of S_C. We allowed for three climate scenarios; in the first, we used the data from 1980–2010 and this will be referred to as the original forcing scenario. In the second, we created a time series of 30 years of forcing by replicating the data from 1990–2000 three times consecutively, hereafter described as the repeated forcing scenario. The third scenario was created by rescaling all precipitation from year 16 onward by a factor of 1.3, implying a 30% increase in precipitation. This was done to determine whether our proposed scheme for identifying wetland consolidation was robust against interdecadal variations in weather. These years were selected to match the timing of the observed consolidation-driven change in the North Dakota (ND) PPR with the appropriate forcing time series.

Our representation of wetlands as conical depressions requires specification of catchment size and slope. To obtain a realistic distribution of topographic gradients and catchment sizes, we used elevation data from the National Elevation Dataset (U.S. Geological Survey, 2009) at a 10-m resolution in a 60 km × 60 km (3,600 km^2) square centered on the location −99.15°W, 47.02°S in Stutsman County, North Dakota. A slope raster was calculated using the Surface Toolbox in ArcGIS 10.2, and a histogram with 1,000 slope value bins from 0.0 (completely flat) to the maximum observed slope of 1.01 (approximately 45° angle) was calculated from the values of this raster. The histogram was normalized to produce an empirical probability distribution function used as the sampling distribution for the per-catchment $Slope_i$. One limitation of this approach is that it assumes that the distribution of average or effective slopes across wetland catchments is similar to that of the per-cell distribution of slopes. A similar approach was used to derive the sampling distribution of the per-catchment area. Next, we estimated a distribution of wetland basin sizes based on the following procedure: all National Wetland Inventory (U.S. FWS, 2016) features with total area greater than 1 ha intersecting the extent of the elevation data used in the previous step. Any overlapping NWI features were combined using the Dissolve and Multipart Split tools in ArcGIS. Before the calculation of basin extent, a preprocessing procedure was applied in which any pixel within an NWI entity was set to be equal to the minimum elevation observed within that entity. This was done to ensure that wetland catchments were not split due to insignificant variations in elevation reported by the NED. We found that omission of this step led to gross underestimation of the frequency of larger catchments. Then, the Flow Direction and Basin tools in the ArcGIS Hydrology Toolbox were applied to the processed elevation raster to delineate the catchments for all topographic depressions, and the subset of these catchments containing an NWI feature with area $>$ 1 ha was identified. Any catchments intersecting the edge of the study area were discarded. The simulation per-catchment area C_i was sampled with replacement from this observed distribution of 2,811 delineated catchment areas. This allows for different combinations of contributing area and stage-area relations as controlled by catchment slope. The water volume for each wetland was converted into a ponded area via (6), which is exact for circular conic catchments and ponded areas.

$$a_i = \pi\left(\frac{3\pi V_i}{\text{Slope}_i}\right)^{\frac{2}{3}} \tag{4}$$

Wetland water volumes and ponded areas were simulated using a mass balance approach. For each wetland, the volume was updated on a daily time step using the following equation:

$$V_{t+1} = V_t + P_t + R_t + D_t^{\text{gain}} + S_t - G_t - D_t^{\text{loss}} - E_t \tag{5}$$

In this equation, the contributions to the water volume are denoted by P_t for direct rainfall onto the ponded area, R_t for nonsnowmelt runoff from the catchment, S_t for snowmelt runoff, and D_t^{gain} for incoming water from an upstream drained wetland. The loss terms are G_t for groundwater losses, E_t for evaporation from the water surface, and D_t^{loss} for water, which is drained out of the wetland. The calculation of all nondrainage terms is followed precisely as laid out in Huang et al. (2013) and is repeated below.

The contribution of direct precipitation to water surface as a function of the ponded area Aa_t and the rainfall rate ρ_t is the product $\rho_t \cdot a_t$. This quantity is dependent on temperature; any precipitation during periods when the air temperature is below zero is instead added to the snowpack. Total evaporation from the ponded area of the wetland is represented in equation (6) in terms of the potential evapotranspiration, the ponded area, and an air temperature indicator I_E. $I_E = 1$ if the trailing mean of the air temperature over the previous 10 days exceeds 3 °C and is 0 otherwise.

$$E_t = \text{PET}_t \cdot a_t \cdot I_E \tag{6}$$

Any precipitation occurring when the air temperature falls below zero is accumulated as snowpack (SP_t) over the entire catchment basin, including the ponded area which is assumed to freeze over. On days when the temperature exceeds zero with existing snowpack on the ground, the snowmelt is calculated in (7) via the degree-day method and this is subtracted from the remaining snowpack. The snowmelt term is nonzero only if the temperature is above zero, corresponding to the condition that the indicator variable $I_T = 1$. To accommodate variability in catchment response to snowmelt runoff, we assigned each catchment a snowmelt capture ratio (CR) at random from 85% to 100%. This parameter controls the fraction of snowmelt that accumulates in the wetland.

$$S_t = \text{CR} \cdot I_T \cdot \text{minimum}(\text{SP}_t, 0.272T_t) \cdot C \tag{7}$$

Deep groundwater loss through wetland bottoms was not considered in this model. All subsurface loss was assumed to be lateral as hydraulic conductivities through wetland bottoms are sufficiently low to preclude substantial vertical loss (van der Kamp & Hayashi, 2009). Lateral loss is represented in equation (8) as a function of a reference recession slope of 0.04 m^2/day S_{RR}, the daily potential evapotranspiration PET_t, a reference evaporation E_R of 4.7 mm/day, and the wetland perimeter p_t. The value of the factor ω was set to be 0.90 as in Huang et al. (2013).

$$G_t = \frac{\omega S_{RR} \text{PET}_t}{E_R} \cdot p_t \tag{8}$$

Rainfall runoff was calculated using the curve number approach (U.S. Soil Conservation Service, 1954) modified to incorporate antecedent moisture. The full details of this derivation are covered in (Huang et al., 2013) and were implemented exactly to that specification. Each watershed was assigned a curve number CN_i at random from 49 to 89 to allow for a range of runoff responses representative of grasslands (CN = 49) to cultivated fields (CN = 89). To allow for the consolidation of wetlands, we incorporated the possibility of drainage. A period of drainage was assumed to run from 1 January 1996 to 1 January 1997 in all simulations. During this period, we considered two cases. In the first, all wetlands had identical probability of being drained, while in the second case, only wetlands with ponded area less than 10 ha were allowed to be drained with equal probability, and all larger wetlands had zero probability of drainage. The second case represents a scenario in which smaller wetlands are more likely to be drained. If a wetland was selected for drainage, a downstream wetland was selected at random from the remaining set of wetlands. The entire

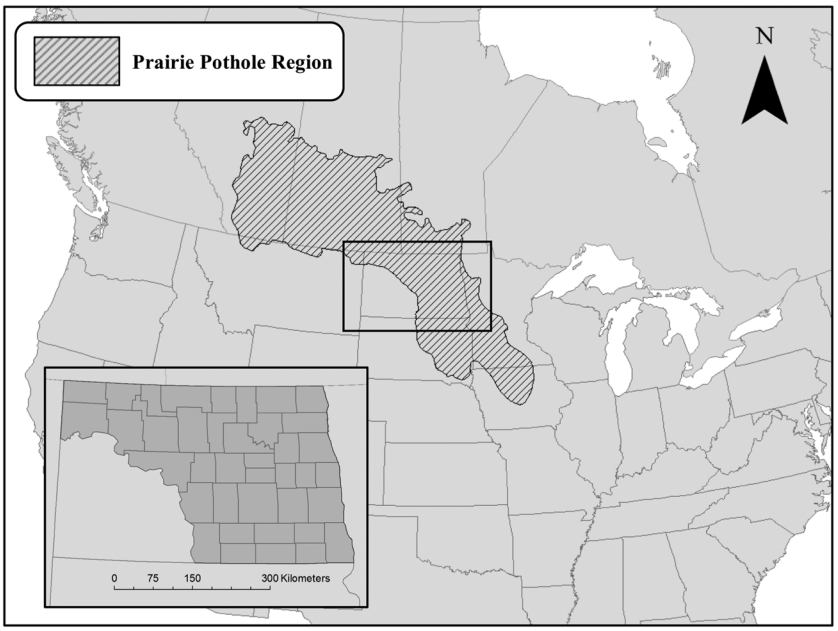

Figure 1. The study area consists of the 38 outlined counties (inset) in North Dakota lying within the North American Prairie Pothole Region.

volume of the upstream wetland then was counted as the drainage loss D_{loss} for the upstream site and was added as the term D_{gain} in the downstream site. A transmission loss for this routed water was sampled for each upstream wetland uniformly as random between 0 and 15%. This controlled the fraction of water lost while flowing from upstream to downstream. While each wetland could be drained only once, there was no restriction on the number of wetlands flowing to the same downstream location.

Time series of water volume for three simulated wetlands are shown in Figure S1. This model required daily data for air temperature, precipitation, and potential evapotranspiration. We used Google Earth Engine to download daily GRIDMET (Abatzoglou et al., 2014) data of these variables from 1 January 1980 to 31 December 2009 for 10 locations in the ND PPR for the locations listed in Table S1. Each landscape-level unit of 1,000 wetlands was driven with the same forcing data randomly assigned from one of the 10 points. In total, we simulated the simplified water balance dynamics for 1.1×10^6 wetlands.

2.3. Remote Sensing Analysis of Ponded Area in the ND PPR

We identified 38 counties in the state of North Dakota in the United States (Figure 1), which partially or wholly intersect the extent of the PPR (Mann, 1974). These counties comprise 132,120 square kilometers and cover the majority of the state and all state land east of the Missouri River.

To identify the location of ponded water in wetlands, we used the Global Surface Water (GSW) data set, which is a collection of raster layers of open water surfaces derived from Landsat 5, 7, and 8 scenes with an expert system for classification. These data are specified at a 30-m. spatial resolution and a monthly temporal resolution. As an extensive global validation process with ground-truth evaluation of approximately 40,000 pixels was conducted in the creation of the GSW data, additional validation was not performed in this study. The original study describing the creation and assessment of this data set (Pekel et al., 2016) listed commission errors corresponding to accuracy of $>$98.4% and errors of omission corresponding to accuracy $>$73.8% for seasonal water and included several hundred ground truth locations within the PPR. All available GSW data over the entire span of 1984–2014 from the months of April to October were retrieved; winter and early springtime observations were unusable due to snow cover and ice. From these data, a derivative layer was created indicating, for each year, all the pixels where water was observed in that year. This aggregated layer was converted into vector format to identify all observable water bodies as polygons for each year 1984–2014. We also calculated the fraction of the study area, which was covered with water for each month April–October for the length of the study period (Figure 2). The number of polygons identified for each year

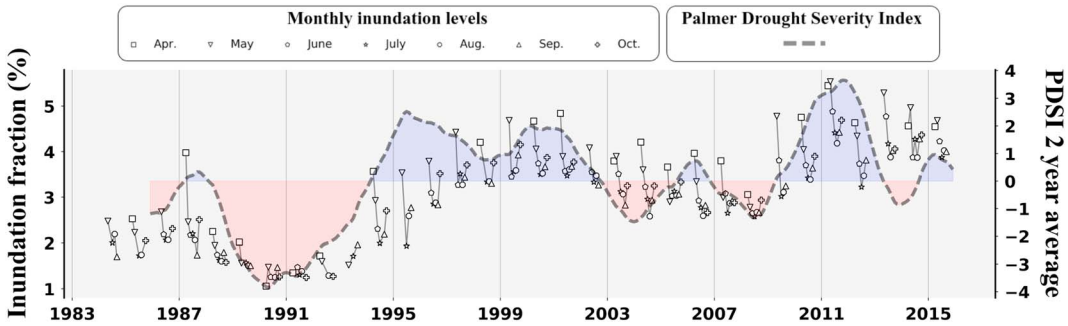

Figure 2. Extent of all inundated area in North Dakota Prairie Pothole Region in relation to Palmer Drought Severity Index. Monthly observations from the same year are connected with a solid black line. Following a major drought from 1988 to 1992, more and more area has been added to water bodies of all types. The inundated area tracks the PDSI with less flooded land in times of drought. Substantial increases in inundated area were observed from 1991 to 2000 and from 2008 to 2012.

varied from a minimum of 4.78×10^5 in 1992 to a maximum of 1.22×10^6 in 1998. We used these polygons to calculate the total area and perimeter of all water bodies for the entire study region and for each county. This was repeated for each year from 1984 to 2014. The proportion of these polygons, which consisted of a single pixel, varied from a maximum of 24.8% in 1989 to a minimum of 18.5% in 2013. We also examined the inundated area for large (≥5 ha) and small water bodies (<5 ha) and plotted these as a function of time in Figure S2. While both categories were overall increasing, the total area in small water bodies grew by approximately 150%, while the area in larger water bodies grew by approximately 75%.

Months for which more than 25% of the study area was unobserved due to missing or incomplete data were omitted. We also analyzed the extent to which GSW observations of water overlap National Wetland Inventory polygons. We calculated the fraction of NWI area, which displayed water at any point from 1984 to 2014 and compiled these results for all ND PPR counties in Table S2. In total, 44.8% of all area within NWI polygons in the ND PPR was also covered with water at some point in time according to the GSW data set. We note that each NWI polygon is, in general, a spatial superset of a ponded area surrounded by a peripheral zone with marsh vegetation and hydric soil. Consequently, it is inevitable that estimates of ponded water extent from GSW are a lower bound on the size of wetlands as estimated by the National Wetland Inventory. In this study, any computational operations performed on vector features and all raster-to-vector conversions were done in Python using the software packages Shapely, Fiona, and GeoPandas. Raster computations were performed in Google Earth Engine.

2.4. Change Point Regression Model

To explore whether there was a substantial shift in the geometries of water bodies over 1984–2014, we created a statistical model relating the annual water area for each year to the annual sum of perimeters. To quantify our uncertainty regarding which year is the most likely change year, we applied a Bayesian change point regression model. This model assumed that the observations of area and perimeter are generated by two linear processes with distinct coefficients and that the observed data are divided into two groups by a single year, designated as the change point year. In practice, this means fitting one linear regression to the *before* period and another to the *after* period, with the year splitting the two periods serving as a latent variable in our model.

Specifically, we modeled $\sqrt{A}_t$, the annual root sum of water areas, as a function of the sum of water perimeters, P_t. We allowed the parameters of this model to change once over the period 1984–2014; the date at which the parameters change is treated as an unknown quantity that must be estimated. The equation for this model is

$$\sqrt{A}_t = I_{t>y_c}(\beta_1 \cdot P_t + \alpha_1) + I_{t\le y_c}(\beta_2 \cdot P_t + \alpha_2) + \epsilon_t \quad (9)$$

where $I_{t<y_c}$ denotes the indicator function, which is equal to 1 if the year is prior to the change point year y_c and 0 otherwise. The error term ϵ_t was assumed to be normally distributed with zero mean and an unknown variance of σ^2. Within this model, there are six parameters to be estimated: the prechange and postchange point linear regression slopes β_1, β_2; the corresponding intercepts α_1, α_2; the error variance σ^2;

Table 1
Summaries of Posterior Estimates of Model Parameters for Change Point Regression and the Optimal Attribution Regression Model

		Parameter	Mean	SD	Lower 2.5%	Upper 97.5%	Eff. samples	$\widehat{R}$
Change point regression	Unrestricted	y_c	1,999	0.81	1,998	2,000	27,424	1.00
		α_1	31,028	946	29,173	32,898	39,378	1.00
		α_2	45,679	2,369	41,034	50,415	6,205	1.00
		β_1	0.000323	0.000011	0.000345	0.000345	31,865	1.00
		β_2	0.000256	0.000022	0.000212	0.000301	6,185	1.00
		σ^2	1,454	206	1,081	1,864	135,539	1.00
	NWI-only	y_c	1,999	0.97	1,997	2,000	30,957	1.00
		α_1	26,929	497	25,948	27,914	43,601	1.00
		α_2	38,902	1,467	36,044	41,808	4,719	1.00
		β_1	0.000295	0.000006	0.000282	0.000307	41,349	1.00
		β_2	0.000208	0.000015	0.000179	0.000237	4,714	1.00
		σ^2	777	110	580	1,000	110,243	1.00
	Attribution regression	ΔWheat	−0.77	0.14	−1.09	−0.53	946	1.00
		ΔDrainage	−0.33	0.15	−0.60	−0.02	926	1.00
		Area_{1985}	0.03	0.13	−0.22	0.30	882	1.00
		α	0.01	0.12	−0.23	0.25	877	1.00
		σ^2	0.6	0.15	0.35	0.90	711	1.00

and the change point year y_c. We estimated all parameters simultaneously using Markov chain Monte Carlo (MCMC) as implemented in PyMC3 (Salvatier et al., 2016), a Bayesian statistical programming framework written primarily in Python. We placed a uniform prior distribution on the change point year y, allowing it to be selected from any year 1986–2013. We placed a Half-Cauchy prior (Polson & Scott, 2012) on the error variance σ^2. This prior consists of a Cauchy distribution centered at zero but truncated to only allow for positive values. Both prechange and postchange periods shared the same error variance. Flat priors were set on the linear regression parameters α_1, α_2, β_1, and β_2. We used the Metropolis-Hastings sampler implemented in PyMC3 and drew 100,000 samples per chain for four chains and discarded the first 20,000 for burn-in. The convergence diagnostic $\widehat{R}$ (Brooks & Gelman, 1998) indicated that the cross-chain correlations were close to the cross-sample correlations and that the chains appeared to be well mixed. Summaries of the posterior distribution for the model parameters are shown in Table 1. More than 6,000 effective samples were obtained from each parameter out of a total Monte Carlo sample size of 400,000 split across four chains.

We assessed the robustness of our analysis by repeating this same analysis for locations that have previously been identified as National Wetland Inventory sites. We obtained shapefiles of all the NWI polygons in North Dakota from the U.S. Fish and Wildlife Service and, for each of 39 counties, computed the intersection between all NWI polygons and the county boundaries to produce a per-county NWI subset. We then expanded the spatial extent of these polygons by applying a 100-m. buffer. This was done to account for possible expansion of water bodies over the past several decades. No distinction was made between types of water bodies or wetlands delineated within the NWI. Next, to calculate the overlap between the GSW-derived polygons and the NWI polygons, we first identified the intersection between the GSW polygons and the county boundary for each county to make the GSW-NWI intersecting analysis parallelizable across counties. Then, we computed the intersection between each county-specific set of NWI polygons and GSW polygons. As this was done for each year, we repeated this task $39 \times 31 = 1209$ times to evaluate the overlap across all counties (39) and all years (31). We were unable to calculate the intersection for three counties (Pembina, Walsh, and Grand Forks) in the NE corner of North Dakota across several years. We suspect that this is due to pathological geometry of the GSW polygons during flooding of the Red River of the North during this time. These missing subsets constitute 19 out of 1209 county-year pairs. We omitted these three counties from the NWI-only change point analysis. We then applied an identical procedure as before to calculate the area and perimeter of water bodies over the entire study area. In both analyses, the estimated change point year fell within the interval (1997, 2000) with 95% posterior probability and a posterior mean of 1999. More extensive discussion of these results is given in section 3.2. We used this estimated change point year of 1999 in the next section to examine the spatial variation in changes measured by S_C.

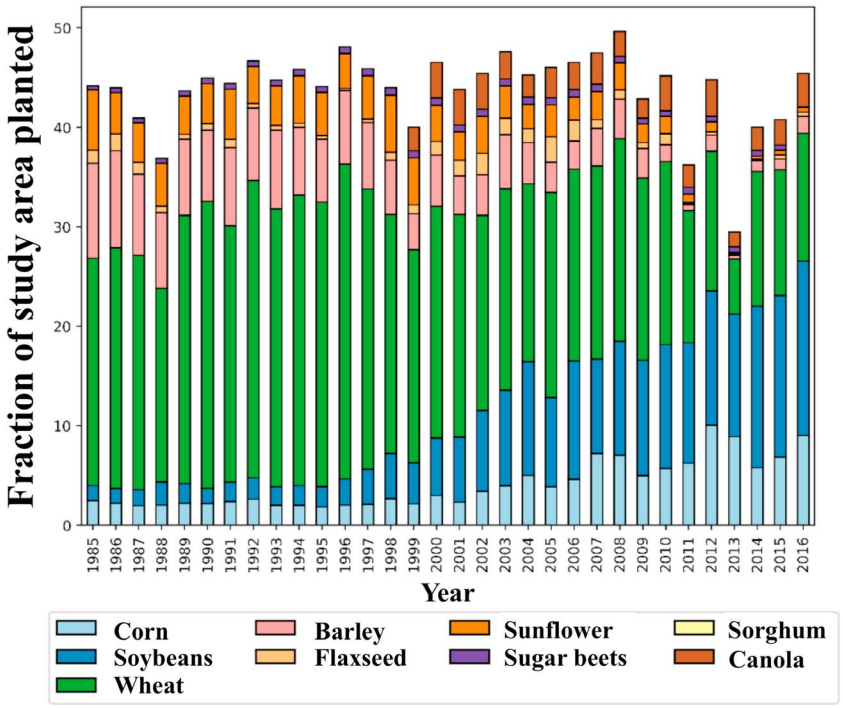

Figure 3. Crop type changes in North Dakota Prairie Pothole Region. Beginning in the early mid-1990s, small grains such as wheat and barley were steadily replaced by corn and soybeans. These data were obtained from the U.S. Department of Agriculture National Agricultural Statistics Service Quick Stats Database.

2.5. Consolidation Attribution Regression Model

We fit the model of the previous section assuming a change date of 1999 to obtain a maximum a posteriori estimates of S_C for each North Dakota county (n = 39) intersecting the PPR. For each of the ND counties, we calculated, for each year, the total perimeter and area of all water polygons intersecting the county. We then calculated S_C for each of these counties.

We then conducted a regression analysis to model S_C as a function of changes in crop type and drainage while controlling for the amount of water present in each county. We accessed NASS records from the U.S. Department of Agriculture (USDA) Quick Stats portal (U.S. Department of Agriculture National Agricultural Statistics Service (USDA-NASS), 2017) and calculated the mean over two periods, 1985–1999 and 2000–2014, of the percentage of each county's land used to grow wheat, corn, or soy. We calculated the difference between these two periods, referred to as ΔWheat, ΔCorn, and ΔSoy. We employed this aggregation over years to minimize the effects of crop rotations or short-term market fluctuations and their impact on crop acreage. The proportion of the study area used to grow corn and soy appeared to be steadily increasing from the mid 1990s-onward (Figure 3).

Next, changes in per-county drainage from the U.S. Census of Agriculture between the years of 1974 and 2012 were compiled in a fashion similar to Kelly et al. (2017). There were no additional years of data available between these time points. The 1974 Census of Agriculture only contained a single survey field for areal extent of land with artificial drainage, while the 2012 Census asked for surface and subsurface drainage separately. We added together surface and subsurface drained areas from the 2012 Census of Agriculture and subtracted the per-county total drained area for 1974 from that of 2012 to arrive at a change in drained area from 1974 to 2012. We then normalized this value by the amount of cropland present in 2012 to calculate a per-county value, which we designate ΔDrainage, the normalized change in artificially drained cropland. Finally, we computed the area of all locations, which were underwater in 1985 on a per-county basis to obtain a control variable, Area_{1985} for the amount of water on the landscape prior to recent consolidation. We included this variable in our regression analyses to attempt to identify any bias in our results due to natural variation in the number of water bodies in different counties.

In our regression analysis, we adopted a two stage procedure. We first enumerated all possible models with no interaction terms. Then, the best performing model was selected and we added an interaction term between the significant covariates to investigate the correlation structure for that model. For the first stage a set of Bayesian linear regression models was constructed with the covariates {ΔWheat, ΔCorn, ΔSoy, ΔDrainage, and Area_{1985}} and response variable S_C defined for each county. All possible models controlling for Area_{1985} and including one or more of the covariate set {ΔWheat, ΔCorn, ΔSoy, and ΔDrainage} with no interactions were considered, for a total of $2^4 - 1 = 15$ models.

Each variable was standardized to have zero mean and unit standard deviation. These were used as predictors of S_C on a per-county level. We found that ΔWheat, ΔCorn,and ΔSoy all covaried (Figure S3); this was not surprising given the ongoing transition from small grains into soy and corn across the northern Great Plains (Johnston, 2014). We placed a half-Cauchy prior on the error variance and fixed its β hyperparameter to be 0.25. A flat prior distribution was assumed for the linear regression coefficients and the intercept. Since this model has a continuous likelihood function unlike the change point model in the previous section, it can be efficiently estimated with MCMC using the No-U-Turn Sampler (NUTS; Hoffman & Gelman, 2014) and we employed NUTS as implemented in PyMC3 to estimate the parameters of this model. For each model, we drew 500 samples per chain after discarding an initial 500 samples. Four chains were computed per model, and these were used to calculate the convergence diagnostic $\widehat{R}$ as in the previous section. We then ranked the models (Table S3) according to the Watanabe-Akaike Information Criterion (WAIC; Watanabe, 2013), which penalizes models with more parameters and favors models with an estimated higher model likelihood. The WAIC-optimal model with no interaction term included ΔWheat and ΔDrainage as predictors in addition to Area_{1985}. The response variable and all predictor variables were centered and standardized to have zero mean and unit standard deviation. In the second stage of our analysis, we refit the optimal model of ΔLS including ΔWheat and ΔDrainage and Area_{1985}, while also adding the interaction term ΔWheat × ΔDrainage as a predictor. This term was included to identify whether or not locations undergoing land use change were sufficiently heterogeneous with regard to drainage application to warrant a more complicated model. We applied the same estimation procedure as before to calculate parameter estimates for this interaction model.

2.6. Limitations

In our observational analysis of PPR wetland ponded extent, we are unable to resolve any water features smaller than the minimum Landsat resolution (900 m^2), which means that many of the smallest pothole wetlands cannot be studied with this approach. As newer sources of satellite imagery are released, it may be possible to employ more advanced statistical or pattern recognition methods to provide a more detailed inventory of the region's water bodies. Classification of shallow water can be especially difficult due to large quantities of suspended sediments or emergent vegetation, and it is likely that many of the water bodies tabulated in our data are underestimated with regard to true areal extent.

The crop and drainage data for our regression analysis is based on USDA surveys and therefore are accurate insofar as the survey responses are accurately compiled. The drainage data we obtained from the 1974 and 2012 Census of Agriculture does not exactly match the temporal span 1984–2014. Furthermore, these data are self-reported and it is possible that farmers are prone to underestimating state the true extent of installed drainage. We did not attempt to calculate the net change in value of ecosystem services provided nor do we attempt to contextualize our results within a larger discussion regarding the advantages and disadvantages of wetland drainage from a food policy or agriculture-centric point of view.

In our hydrology simulations, we restricted our analysis to conical wetland basins to control for the effect of variation in basin irregularity and elongation; however, this does lead to a resulting drainage-consolidation relation, which may be different than what is actually observed. Consequently, we cannot attempt to back out estimates of drainage prevalence from the values of S_C derived from remote sensing data. The model we implemented simplifies or omits many processes such as infiltration through the basin bottom or fill/spill merging of wetlands. The representation of snowpack with uniform depth and melt rates is also a simplification as snowpack can vary dramatically depending on local topographic and land cover characteristics (Pomeroy et al., 1993). Additionally, our representation of artificial drainage is simplistic. A more realistic

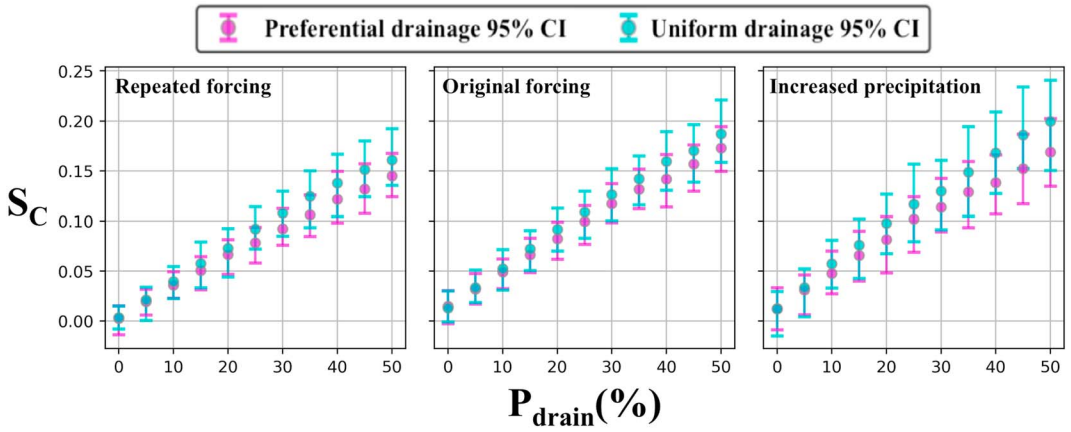

Figure 4. Simulated effect of wetland consolidation on the consolidation score S_C. In each landscape unit of 1,000 wetland catchments, the intensity of drainage was controlled by P_{drain} and the resulting values of S_C were tabulated. Markers indicate simulation medians.

model would incorporate water fluxes due to drainage as a function of soil moisture and some notion of proximity of drainage channels to ponded water as was done in Amado et al. (2016) and Werner et al. (2016).

3. Results

3.1. Hydrologic Simulations

The intent of this analysis was to determine whether the quantity S_C covaried with the intensity of agricultural drainage and/or with natural climatic variation in precipitation and temperature. Consequently, we were interested in determining the value of S_C when no drainage was applied ($P_{drain} = 0$). Figure 4 shows the results for this case and for higher values of P_{drain}, indicating that S_C is approximately zero when no drainage is applied. Given that the original simulation used forcing data from the exact period that used in our observational study (section 2.2), it appears that the natural variation in precipitation and temperature is not sufficient to cause noticeable changes in shape index as tabulated by S_C. Furthermore, the scenario corresponding to increased precipitation in the latter half of the simulation also showed a zero value for S_C. In all scenarios, S_C scales linearly with increasing drainage. This suggests that it is sensitive to agricultural drainage and that aggregating many small water bodies into a few larger ones leads to a change to landscape-level shape index that can be observed. However, there was little distinction between the preferential and uniform drainage scenarios; the former favored drainage of smaller water bodies, while the latter applied the same probability of drainage to all water bodies.

In a realistic landscape, the effect of drainage on S_C could be mediated by changes in the size distribution of wetlands or by alterations to wetland morphologies, that is, long, skinny wetlands being consolidated into more regular shapes. Given that each simulated wetland was assumed to have a circular ponded area, the effect of drainage on S_C must be due to changes in the size distribution or the number of wetlands as morphological changes were not allowed in this simulation. With these results, we are confident that wetland consolidation covaries with S_C and that this latter quantity appears to be independent of simple increases in precipitation. However, as we did not account for the geometric effects of compactification and consolidation of ponded areas, the results from these numerical simulations are only a rough approximation of what is observed in real landscapes. Furthermore, there may exist additional potential confounding factors leading to changes in LS, which we have not considered.

3.2. Change Point Regression Model

Calculation of S_C per equation (3) requires demarcating two disjoint time periods. A plot of $\sqrt{A_t}$ versus P_t showed a clear structural shift between two apparently linear relations which roughly correspond to data before and after 1999 (Figure 5).

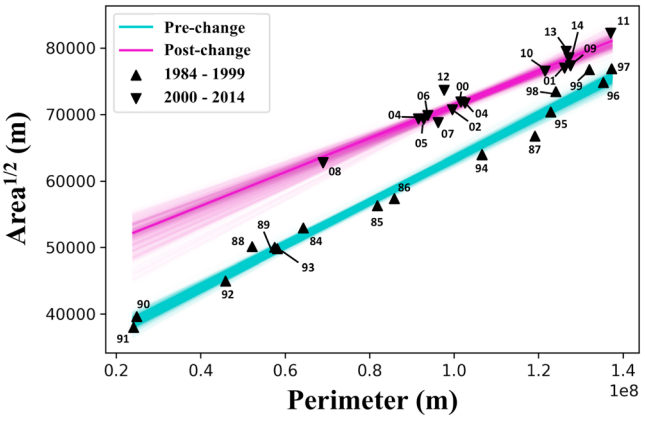

Figure 5. Consolidation in area-perimeter relation. Each point represents $\sqrt{A}$ and P for a single year. Individual points are labeled by the last two digits of the year, that is, 84 for 1984 and 02 for 2002. The alteration of distribution of water body sizes induced by wetland consolidation manifests as a shift from one area-perimeter relation as shown in teal to a new functional relation as indicated in purple. Each line shown above is a linear regression based on a single sample from our Bayesian estimation procedure. The data shown are derived from calculations over the entire North Dakota Prairie Pothole Region. The most likely dates of change in the area-perimeter relation (1998, 1999) as judged from this plot appear to lie in between the two estimated per-period relations.

Summaries of the posterior distribution for the model parameters are shown in Table 1. For the model parameter indicating the change point year, posterior probability mass was concentrated on the years 1998 and 1999 with a smaller portion showing support for 2000. These results indicate strong support for the hypothesis that structural changes to ND PPR area-perimeter relations took place around the year 1999. Furthermore, the low residual variance suggests that this is an appropriate representation of the data. We repeated this analysis with the intersection of the GSW-derived water polygons with all NWI polygons buffered by 100 m to assess whether this result was still valid when considering only locations previously identified as wetlands in the National Wetland Inventory. With this added constraint, we found that the most likely year for change was again 1999, though the 95% credible interval also included the year 1997 as well.

3.3. Consolidation Attribution Regression Model

The spatial distribution of S_C can be seen in Figure S5, and this pattern indicates relatively little change in the far northwest of the state and the Red River Valley in the east. This distribution indicates that the statewide shift in area-perimeter relation is not due to the expansion or consolidation of water bodies in any single county.

To convey the predictive ability of the regression models of S_c in a familiar way, we employ the Bayesian R^2 (Gelman et al., 2017) as an analogue of the frequentist quantity of the same name. Instead of computing a single value for R^2 we instead obtain a distribution of R^2 values, each corresponding to a single sample from the predictive posterior distribution. The optimal no-interaction model had a median R^2 of 0.48 with standard deviation of 0.07 and the interaction model had a median R^2 of 0.49 with standard deviation of 0.07. The Monte Carlo estimates of the model coefficients are shown in Table 1. As the interaction model WAIC (97.72) was not an improvement over the optimal no-interaction model (WAIC = 96.76) we did not conduct analysis of its coefficients. The optimal no-interaction model had coefficients for wheat and drainage, which excluded zero from their 95% credible intervals, and therefore, these covariates appear to be important. However, the sign of the drainage coefficient is contrary to what would be expected from the hypothesis that drainage alone is responsible for large values of S_C. The signs on both the coefficient linking change in area farmed for wheat and the estimated increase in drainage are both anticorrelated with increasing values of S_C.

4. Discussion

Artificial manipulation of wetlands can affect wetland geometries and area/perimeter relations in at least two ways; drainage typically leads to more compact geometries with shortened perimeters. Additionally, removing wetlands from the landscape reduces LS by simply reducing the number of terms in the sum in equation (2). While we are unable to determine which of these effects dominates, it is apparent that a major structural shift in the region-wide area/perimeter ratio occurred around 1999–2000. This comes just 2 years after widespread flooding in the spring of 1997 (Todhunter, 2001) and a wet period following a lengthy drought, which terminated in the early 1990s (Todhunter, 2016). The amount of land underwater attained a near-maximum between 2000 and 2002 (Figure 2) with more inundation only coming over a decade later in 2011–2013.

Given that the shift in LS observed in 1999 also coincided with a period with a large amount of water stored on the landscape, these data suggest a major hysteretic effect in the area-perimeter relationship as depicted in Figure 6. Such an interpretation fits coherently with an attribution to anthropogenic causes; widespread overland flooding could potentially lead to installation of surface drainage to keep farmland arable. McKenna et al. (2017) determined that installations of subsurface drainage did not substantially increase until after 2003 on the basis of North Dakota State Water Commission permit data (Finocchiar, 2014), but that data set does not include surface drainage and is also limited to listing permits for subsurface drainage projects

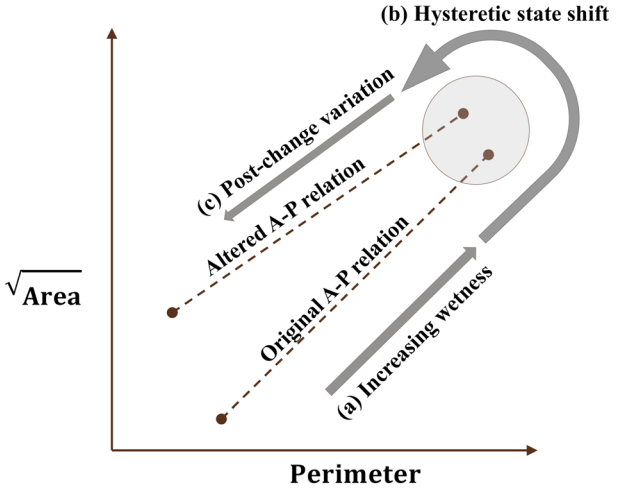

Figure 6. Hysteresis in area-perimeter relation. As more and more water is accumulated on the landscape (a), the system approaches a limit or breakpoint at which either natural or anthropogenic effects (b) cause the post-change area-perimeter relation to be structurally different than before. Increased surface areas for the same perimetric length indicate that water is being stored in either larger or more compact water bodies and in the new regime (c), natural filling, and emptying cycles correspond to movement along the new A-P function.

over 80 acres (32.37 ha). In light of these facts, we opine that we cannot conclusively rule out the possibility of extensive, widespread surface drainage around the year 1999 on the basis of the findings in McKenna et al. (2017).

An alternative hypothesis is that these are shifts incurred by dramatic increases in precipitation and that anthropogenic manipulation was relatively unimportant. However, this does not explain why there exists a strong correlation between changes in crop type and large values of S_C (Table 1), as increases in rainfall were noted to take place across the entire region and are unlikely to provide a common cause for changes in both of these variables. Simply increasing the amount of water stored on the landscape does not appear to be a sufficient condition for changes in the area-perimeter relation which we observed. Our investigation into the suitability of S_C for tracking changes in wetland size distribution revealed that natural drying/filling cycles are unlikely to lead to dramatic changes in landscape-wide $\frac{\sqrt{A}}{P}$ ratios on their own. A consistent increase in rainfall over the years 1993–2000 did indeed lead to the formation and flooding of numerous new water bodies as evidenced by increases in inundated area (Figure 2), but the landscape-level shape index, that is, the slope and intercept of the area$^{1/2}$ and perimeter relation, did not appreciably change over this time period but did change substantially post-1999 (Figure 5). This fact also appears to rule out an explanation contained within a study by Kahara et al. (2009), which described the expansion and merging of wetlands between 1979–1986 and 1995–1999, finding that smaller, more isolated wetlands *disappear* due to merging with larger water bodies nearby. This is understood to be a reversible phenomenon in the sense that the landscape-level perimeter and area should return back to the original state after a period of normal or below-normal precipitation. However, this is at odds with our observation that there has been a clear, change in the area-perimeter relation for the ND PPR, which is not reversible via normal interannual variations in precipitation. With regard to direct attribution of this change with regression, we do not have drainage data closer to the year 1999 and it is not clear whether the anticorrelation of reported drainage and consolidation is a truly meaningful relation or if there are issues with either reporting or timing in the Census of Agriculture survey. A superior measure of drainage would be data estimated from either surface topographical data of ditches or remotely sensed soil moisture.

Regardless of the causes leading to the observed change in $\sqrt{A}$-P functional relations, it is clear that the ND PPR has shifted to a new state in which the same amount of inundated area provides substantially reduced perimetric length and accordingly less shoreline habitat. The notion of a state shift has been explored in the literature (McKenna et al., 2017) albeit from the perspective of wetland salinity and hydroclimatic forcing. A central point of McKenna et al. (2017) is that major increases to precipitation may have initiated broad changes in wetland characteristics and this shift was strengthened and exacerbated by land use practices. We view this hypothesis as entirely consistent with our findings as increases in soil moisture would reasonably lead to increased surface ditching or tile installation. However, McKenna et al. states that substantial land use change did not take place between the early 1990s through 2006, while NASS statistics of land use over the entire ND PPR (Figure 6) indicate that dramatic changes in crop type have, in fact, been taking place beginning in the mid 1990s. As this work found strong spatial correlations between the intensity of this state shift and a more refined measure of land use change, we suggest that the phenomenon observed in McKenna et al. is potentially manifest in this work as well. A promising direction for future work is the integration of the remote sensing analyses conducted here with existing work on characterizing state shifts in wetland systems (Mushet et al., 2018) with measurements of salinity as done in McKenna et al. (2017).

The analytical framework outlined here in terms of wetland area and perimeter is transferable to regions, which contain many water bodies lacking surface connections to a stream network. The key assumption, which must be met, is that conservation of mass dictates that any drained water must eventually reach a terminal receiving basin. Then, expanding and shrinking water bodies may reside in close proximity and

we hold this to be a key signature of anthropogenic manipulation. In areas where it is possible to connect artificial drainage channels to a larger stream network, then the methods outlined here are not applicable.

5. Conclusion

In this study we incorporated several sources of agricultural and water data to analyze an observed state shift in landscape-level shape index of wetlands across the North Dakota PPR. We found evidence that a structural shift in area-perimeter relations occurred around the years 1997–2000, and we hypothesize that this may be a hysteretic effect involving anthropogenic and meteorological effects. We performed an additional regression to analyze the covariation of this shift's intensity with changes in crop type and found that a transition out of wheat into corn and soy was highly correlated with the state shift, though available drainage data show a weak anticorrelation with wetland consolidation. We observed that wetland state shifts are occurring and that they are likely tied to both precipitation and land use. Further analysis and more detailed data will be needed to more closely examine the correlation structure between land use and widespread changes in area-perimeter relations. A major challenge for wetland scientists studying the effect of changing land management practices in the PPR is the absence of high-quality and spatially explicit data on all sources of artificial drainage across the region. We hope that this work will encourage further studies integrating data from a range of sources to shed light on ongoing changes to wetlands across the interior of North America.

Acknowledgments

We would like to thank Mike Anteau of the U.S. Geological Survey and Ron Reynolds (ret.) of the U.S. Fish and Wildlife Service for useful discussions and feedback on this work. This research was funded by NASA via the Earth and Space Sciences Fellowship program and the National Science Foundation via an IGERT traineeship through Duke WiSeNet. Additional financial support was provided as by the Duke University Wetland Center. Nvidia provided support for this project via the GPU Grant Program. Coauthor Mukesh Kumar also acknowledges support from National Science Foundation grants EAR-1331846 and EAR-1454983. The data used in this study can be obtained via Google Earth Engine and the USDA NASS Quick Stats online portal.

References

Abatzoglou, J. T., Barbero, R., Wolf, J. W., & Holden, Z. A. (2014). Tracking interannual streamflow variability with drought indices in the U.S. Pacific Northwest. *Journal of Hydrometeorology*, *15*(5), 1900–1912. https://doi.org/10.1175/JHM-D-13-0167.1

Amado, A. A., Politano, M., Schilling, K., & Weber, L. (2016). Investigating hydrologic connectivity of a drained Prairie Pothole Region wetland complex using a fully integrated, physically-based model. *Wetlands*, *38*(2), 233–245. https://doi.org/10.1007/s13157-016-0800-5

Anteau, M. J. (2012). Do interactions of land use and climate affect productivity of Waterbirds and prairie-pothole wetlands? *Wetlands*, *32*(1), 1–9. https://doi.org/10.1007/s13157-011-0206-3

Bluemle, J. (2016). *North Dakota's Geologic Lgeacy: Our land and how it formed*. Fargo, ND: North Dakota State University Press.

Brooks, S. P., & Gelman, A. (1998). General methods for monitoring convergence of iterative simulations. *Journal of Computational and Graphical Statistics*, *7*(4), 434–455. https://doi.org/10.2307/1390675

Calhoun, A. J. K., Mushet, D. M., Alexander, L. C., DeKeyser, E. S., Fowler, L., Lane, C. R., et al. (2017). The significant surface-water connectivity of "geographically isolated wetlands". *Wetlands*, *37*, 801–806. https://doi.org/10.1007/s13157-017-0887-3

Christensen, J., Nash, M., Chaloud, D., & Pitchford, A. (2016). Spatial distributions of small water body types in modified landscapes: Lessons from Indiana, USA. *Ecohydrology*, *9*(1), 122–137. https://doi.org/10.1002/eco.1618

Cohen, M. J., Creed, I. F., Alexander, L., Basu, N. B., Calhoun, A. J. K., Craft, C., et al. (2016). Do geographically isolated wetlands influence landscape functions? *Proceedings of the National Academy of Sciences*, *113*(8), 1978–1986. https://doi.org/10.1073/pnas.1512650113

Cox, J., Hanson, M. A., Roy, C. C., Euliss, J., Johnson, D. H., & Butler, M. G. (1998). Mallard duckling growth and survival in relation to aquatic invertebrates. *Journal of Wildlife Management*, *62*(1), 124–133. https://doi.org/10.2307/3802270

Creed, I. F., Lane, C. R., Serran, J. N., Alexander, L. C., Basu, N. B., Calhoun, A. J. K., et al. (2017). Enhancing protection for vulnerable waters. *Nature Geoscience*, *10*(11), 809–815. https://doi.org/10.1038/ngeo3041

Dahl, T. E. (2014). *Status and trends of prairie wetlands in the United States 1997 to 2009*. Washington, DC: U.S. Department of the Interior; Fish and Wildlife Service, Ecological Services.

Euliss, N. H., Gleason, R. A., Olness, A., McDougal, R. L., Murkin, H. R., Robarts, R. D., et al. (2006). North American prairie wetlands are important nonforested land-based carbon storage sites. *Science of the Total Environment*, *361*(1-3), 179–188. https://doi.org/10.1016/j.scitotenv.2005.06.007

Euliss, N. H., LaBaugh, J. W., Fredrickson, L. H., Mushet, D. M., Laubhan, M. K., Swanson, G. A., et al. (2004). The wetland continuum: A conceptual framework for interpreting biological studies. *Wetlands*, *24*(2), 448–458. https://doi.org/10.1672/0277-5212(2004)024[0448:TWCACF]2.0.CO;2

Finocchiar, R. G. (2014). Agricultural subsurface drainage tile locations by permits in North Dakota. https://doi.org/10.5066/F7QF8QZW

Gelman, A., Goodrich, B., Gabry, J., & Ali, I. (2017). R-squared for Bayesian regression models*.

Hartig, E. K., Grozev, O., & Rosenzweig, C. (1997). Climate change, agriculture and wetlands in Eastern Europe: Vulnerability, adaptation and policy. *Climatic Change*, *36*(1/2), 107–121. https://doi.org/10.1023/A:1005304816660

Hayashi, M., van der Kamp, G., & Rosenberry, D. O. (2016). Hydrology of prairie wetlands: Understanding the integrated surface-water and groundwater processes. *Wetlands*, *36*(S2), 237–254. https://doi.org/10.1007/s13157-016-0797-9

Hoffman, M. D., & Gelman, A. (2014). The no-U-turn sampler: Adaptively setting path lengths in Hamiltonian Monte Carlo. *Journal of Machine Learning Research*, *15*, 1593–1623.

Huang, S., Young, C., Abdul-Aziz, O. I., Dahal, D., Feng, M., & Liu, S. (2013). Simulating the water budget of a Prairie Potholes complex from LiDAR and hydrological models in North Dakota, USA. *Hydrological Sciences Journal*, *58*(7), 1434–1444. https://doi.org/10.1080/02626667.2013.831419

Huang, S., Young, C., Feng, M., Heidemann, K., Cushing, M., Mushet, D. M., & Liu, S. (2011). Demonstration of a conceptual model for using LiDAR to improve the estimation of floodwater mitigation potential of Prairie Pothole Region wetlands. *Journal of Hydrology*, *405*(3-4), 417–426. https://doi.org/10.1016/j.jhydrol.2011.05.040

Johnson, W. C., Boettcher, S. E., Poiani, K. A., & Guntenspergen, G. (2004). Influence of weather extremes on the water levels of glaciated prairie wetlands. *Wetlands*, *24*(2), 385–398. https://doi.org/10.1672/0277-5212(2004)024[0385:IOWEOT]2.0.CO;2

Johnson, W. C., Werner, B., Guntenspergen, G. R., Voldseth, R. A., Millett, B., Naugle, D. E., et al. (2010). Prairie wetland complexes as landscape functional units in a changing climate. *Bioscience*, *60*(2), 128–140. https://doi.org/10.1525/bio.2010.60.2.7

Johnston, C. A. (2013). Wetland losses due to row crop expansion in the Dakota Prairie Pothole Region. *Wetlands*, *33*(1), 175–182. https://doi.org/10.1007/s13157-012-0365-x

Johnston, C. A. (2014). Agricultural expansion: Land use shell game in the U.S. Northern Plains. *Landscape Ecology*, *29*(1), 81–95. https://doi.org/10.1007/s10980-013-9947-0

Kahara, S. N., Mockler, R. M., Higgins, K. F., Chipps, S. R., & Johnson, R. R. (2009). Spatiotemporal patterns of wetland occurrence in the Prairie Pothole Region of eastern South Dakota. *Wetlands*, *29*(2), 678–689. https://doi.org/10.1672/07-09.1

Kantrud, H., Krapu, G., & Swanson, G. (1989). Prairie basin wetlands of the Dakotas: A community profile (Biological Report No. 85). US Fish and Wildlife Service, Northern Prairie Wildlife Research Center.

Kelly, S. A., Takbiri, Z., Belmont, P., & Foufoula-Georgiou, E. (2017). Human amplified changes in precipitation-runoff patterns in large river basins of the Midwestern United States. *Hydrology and Earth System Sciences*, *21*(10), 5065–5088. https://doi.org/10.5194/hess-21-5065-2017

Kessler, A. C., & Gupta, S. C. (2015). Drainage impacts on surficial water retention capacity of a prairie pothole watershed. *JAWRA Journal of the American Water Resources Association*, *51*(4), 1101–1113. https://doi.org/10.1111/jawr.12288

LaBaugh, J. W., Mushet, D. M., Rosenberry, D. O., Euliss, N. H., Goldhaber, M. B., Mills, C. T., & Nelson, R. D. (2016). Changes in pond water levels and surface extent due to climate variability alter solute sources to closed-basin prairie-pothole wetland ponds, 1979 to 2012. *Wetlands*, *36*(S2), 343–355. https://doi.org/10.1007/s13157-016-0808-x

Leibowitz, S. G., Wigington, P. J., Schofield, K. A., Alexander, L. C., Vanderhoof, M. K., & Golden, H. E. (2018). Connectivity of streams and wetlands to downstream waters: An integrated systems framework. *Journal of the American Water Resources Association*, *54*(2), 298–322. https://doi.org/10.1111/1752-1688.12631

Leitch, J. A., & Hovde, B. (1996). Empirical valuation of prairie potholes: Five case studies. *Great Plains Research*, *6*, 16.

Mann, G. E. (1974). The Prairie Pothole Region—A zone of environmental opportunity. *Natura*, *25*, 2–7.

McCauley, L. A., Anteau, M. J., & Post van der Burg, M. (2015). Consolidation drainage and climate change may reduce Piping Plover habitat in the Great Plains. *Journal of Fish and Wildlife Management*, *7*(1), 4–13. https://doi.org/10.3996/072015-JFWM-068

McCauley, L. A., Anteau, M. J., van der Burg, M. P., & Wiltermuth, M. T. (2015). Land use and wetland drainage affect water levels and dynamics of remaining wetlands. *Ecosphere*, *6*, 1–22.

McGarigal, K., & Marks, B. (1994). FRAGSTATS: Spatial pattern analysis program for quantifying landscape structure.

McKenna, O. P., Mushet, D. M., Rosenberry, D. O., & LaBaugh, J. W. (2017). Evidence for a climate-induced ecohydrological state shift in wetland ecosystems of the southern Prairie Pothole Region. *Climatic Change*, *145*(3-4), 273–287. https://doi.org/10.1007/s10584-017-2097-7

Merendino, M. T., & Ankney, C. D. (1994). Habitat use by mallards and American black ducks breeding in Central Ontario. *The Condor*, *96*(2), 411–421. https://doi.org/10.2307/1369324

Mushet, D. M., McKenna, O. P., LaBaugh, J. W., Euliss, N. H., & Rosenberry, D. O. (2018). Accommodating state shifts within the conceptual framework of the wetland continuum. *Wetlands*, *38*(3), 647–651. https://doi.org/10.1007/s13157-018-1004-y

Paradeis, B. L., DeKeyser, E. S., & Kirby, D. R. (2010). Evaluation of restored and native Prairie Pothole Region plant communities following an environmental gradient. *Natural Areas Journal*, *30*(3), 294–304. https://doi.org/10.3375/043.030.0305

Patton, D. R. (1975). A diversity index for quantifying habitat "edge". *Wildlife Society Bulletin*, *3*, 171–173.

Pavelis, G. A. (1987). Farm drainage in the United States: History, status, and prospects. US Department of Agriculture, Economic Research Service.

Pekel, J.-F., Cottam, A., Gorelick, N., & Belward, A. S. (2016). High-resolution mapping of global surface water and its long-term changes. *Nature*, *540*(7633), 418–422. https://doi.org/10.1038/nature20584

Polson, N. G., & Scott, J. G. (2012). On the half-Cauchy prior for a global scale parameter. *Bayesian Analysis*, *7*(4), 887–902. https://doi.org/10.1214/12-BA730

Pomeroy, J. W., Gray, D. M., & Landine, P. G. (1993). The prairie blowing snow model: Characteristics, validation, operation. *Journal of Hydrology*, *144*(1-4), 165–192. https://doi.org/10.1016/0022-1694(93)90171-5

Reynolds, R. E., Shaffer, T. L., Loesch, C. R., & Cox, J. (2006). The Farm Bill and duck production in the Prairie Pothole Region: Increasing the benefits. *Wildlife Society Bulletin*, *34*(4), 963–974. https://doi.org/10.2193/0091-7648(2006)34[963:TFBADP]2.0.CO;2

Salvatier, J., Wiecki, T. V., & Fonnesbeck, C. (2016). Probabilistic programming in Python using PyMC3. *PeerJ Computer Science*, *2*, e55. https://doi.org/10.7717/peerj-cs.55

Serran, J. N., Creed, I. F., Ameli, A. A., & Aldred, D. A. (2018). Estimating rates of wetland loss using power-law functions. *Wetlands*, *38*(1), 109–120. https://doi.org/10.1007/s13157-017-0960-y

Steele, M. K., & Heffernan, J. B. (2017). Land use and topography bend and break fractal rules of water body size-distributions. *Limnology and Oceanography Letters*, *2*(3), 71–80. https://doi.org/10.1002/lol2.10038

Todhunter, P. E. (2001). A hydroclimatological analysis of the Red River of the north snowmelt flood catastrophe of 1997. *JAWRA Journal of the American Water Resources Association*, *37*(5), 1263–1278. https://doi.org/10.1111/j.1752-1688.2001.tb03637.x

Todhunter, P. E. (2016). Mean hydroclimatic and hydrological conditions during two climatic modes in the Devils Lake Basin, North Dakota (USA). *Lakes & Reservoirs: Research & Management*, *21*(4), 338–350. https://doi.org/10.1111/lre.12152

US FWS (2016). NWI program overview [WWW Document]. Retrieved from http://www.fws.gov/wetlands/NWI/Overview.html, (accessed 2.1.16).

USDA-NASS (2017). National Agricultural Statistics Service Quick Stats [WWW Document]. Retrieved from https://www.nass.usda.gov/Quick_Stats/, (accessed 6.20.17).

U.S. Soil Conservation Service (1954). Section 4. Hydrology. In *US Soil Conservation Service* (Chap. 21, section 4, pp. 21.1–21.8). Washington, DC: Government Printing Office. Retrieved from https://directives.sc.egov.usda.gov/OpenNonWebContent.aspx?content=18393.wba

van Asselen, S., Verburg, P. H., Vermaat, J. E., & Janse, J. H. (2013). Drivers of wetland conversion: A global meta-analysis. *PLoS One*, *8*(11), e81292. https://doi.org/10.1371/journal.pone.0081292

van der Kamp, G., & Hayashi, M. (2009). Groundwater-wetland ecosystem interaction in the semiarid glaciated plains of North America. *Hydrogeology Journal*, *17*(1), 203–214. https://doi.org/10.1007/s10040-008-0367-1

Van Meter, K. J., & Basu, N. B. (2015). Signatures of human impact: Size distributions and spatial organization of wetlands in the Prairie Pothole landscape. *Ecological Applications*, *25*(2), 451–465. https://doi.org/10.1890/14-0662.1

Verhoeven, J. T. A., & Setter, T. L. (2010). Agricultural use of wetlands: Opportunities and limitations. *Annals of Botany*, *105*(1), 155–163. https://doi.org/10.1093/aob/mcp172

Watanabe, S. (2013). A widely applicable Bayesian information criterion. *Journal of Machine Learning Research*, *31*.

Werner, B., Tracy, J., Johnson, W. C., Voldseth, R. A., Guntenspergen, G. R., & Millett, B. (2016). Modeling the effects of tile drain placement on the hydrologic function of farmed prairie wetlands. *JAWRA Journal of the American Water Resources Association*, *52*(6), 1482–1492. https://doi.org/10.1111/1752-1688.12471

Wiltermuth, M. T., & Anteau, M. J. (2016). Is consolidation drainage an indirect mechanism for increased abundance of cattail in northern prairie wetlands? *Wetlands Ecology and Management*, *24*(5), 533–544. https://doi.org/10.1007/s11273-016-9485-z

Wright, C. K., & Wimberly, M. C. (2013). Recent land use change in the Western Corn Belt threatens grasslands and wetlands. *Proceedings of the National Academy of Sciences*, *110*(10), 4134–4139. https://doi.org/10.1073/pnas.1215404110

Zhang, B., Schwartz, F. W., & Liu, G. (2009). Systematics in the size structure of prairie pothole lakes through drought and deluge. *Water Resources Research*, *45*, W04421. https://doi.org/10.1029/2008WR006878